Preprints of the 21st IFAC World Congress (Virtual)
Berlin, Germany, July 12-17, 2020

Aircraft Vision-Based Landing Using Robust Extended Command Governors

Laurent Burlion * **Ilya Kolmanovsky** **

* *Rutgers University (e-mail: laurent.burlion (at) rutgers.edu), Piscataway, NJ, USA*
** *University of Michigan, Ann Arbor, MI, USA*

Abstract: We propose a novel vision-based constrained control solution to execute aircraft landing on an unknown runway. The method is based on an extended command governor which is tailored for a specific class of constrained linear systems with a single uncertain modeling parameter. The computational burden is reduced by exploiting a robust strongly returnable set in place of a robust invariant set and computing this set through the use of a binomial expansion. Numerical results illustrate the ability to 'safely' align the aircraft with the runway while satisfying the specified terminal constraints to execute the flare. Here the terminal constraints are efficiently handled by transforming them into time-varying constraints.

Keywords: Constrained control, vision based control, aircraft flight control.

1. INTRODUCTION

Reference and command governors are add-on control schemes that enforce constraints in closed-loop systems (see Kolmanovsky et al. (2012)). Recently, extended command governors (ECG) were introduced by Gilbert and Ong (2011) to enlarge the domain of attraction while retaining the conventional reference governors features. Fewer results are available on reference governors in the case of systems with parametric uncertainties. See, for instance Casavola et al. (2000). Notably, most of governor schemes exploit constraint admissible invariant sets following Gilbert and Tan (1991); Gilbert and Kolmanovsky (2002), and techniques have been developed to efficiently compute such sets for uncertain linear systems (Pluymers et al. (2005)). Mixed logical dynamical (MLD) constraints (Bemporad and Morari (1999)) can represent state dependent terminal conditions and invariant sets can also be computed in this context (see Rakovic et al. (2004)) even though computations and the implementation of the resulting reference governors could be non-trivial. Progress has been made in recent years to efficiently deal with time-varying references (Di Cairano and Borrelli (2016)) and/or constraints (Kalabić and Kolmanovsky (2014)) which in certain situations, such as the one of this paper, can be used to replace MLD constraints.

The developments in this paper are motivated by the aircraft vision based landing problem studied in Gibert et al. (2015); Burlion and de Plinval (2017b) in which the system has a single uncertain parameter. Although not considered in these papers, the align phase would require some terminal constraints in practice in order to properly perform the flare phase. A fast robust reference governor solution for this problem will be developed exploiting a binomial formula for the state transition matrix and the transformation of the terminal constraints into time-varying constraints to efficiently compute some strongly returnable sets (as defined in Gilbert and Kolmanovsky (2002)).

This paper is organized as follows. In Section II, we describe our approach to compute a robust invariant set based on the binomial formula. We then apply this technique to the design of a robust ECG to control a constrained aircraft landing in Section III. Numerical results are reported in Section IV. Simulations based on a nonlinear continuous-time model are also included to validate our design based on linearized discrete-time models. Section V presents concluding remarks.

The following notations are used:
$\underset{k\in\{1,n\}}{Co}\{A_k\} = Co\{A_1, A_2, ..., A_n\}$ denotes the convex hull of matrices A_1,A_2 ... and A_n.
The standard unit simplex in $\mathbb{R}^2$ is given by:

$$\mathscr{P}_2 := \{p \in \mathbb{R}^2 : p_1 + p_2 = 1; p_1 \geq 0; p_2 \geq 0\} \quad (1)$$

2. FAST ROBUST ECG SYNTHESIS

The objective of this section is to extend the conventional Extended Command Governors (ECG) scheme to systems with a single uncertain parameter while limiting the computational footprint. In subsection 2.1, we review the design of ECG based on the computation of the maximal output admissible set O_∞ ; then, in subsection 2.2, we propose to use a binomial formula to efficiently compute a subset of O_∞ in place of O_∞ in case the system dynamics are uncertain. Such a subset is no longer invariant but still allows to synthetize an ECG.

2.1 Preliminaries on conventional ECG

We first review the basics of the conventional ECG introduced in Gilbert and Ong (2011). These schemes enjoy the same properties as the classical reference governors (RG) but outperform them by providing a faster response and enlarging the constrained domain of attraction. For this the ECG exploits the extra degrees of freedom offered by the use of an auxiliary subsystem, the state of which can be reset when necessary to enforce the constraints.

Consider the following class of time-invariant discrete-time linear systems:

$$\begin{aligned} x(k+1) &= Ax(k)+Bv(k), \\ y(k) &= Cx(k)+Dv(k), \end{aligned} \tag{2}$$

in which $k \in \mathbb{Z}^+$, $x(k) \in \mathbb{R}^{n_x}$ is the plant state, $v(k) \in \mathscr{R}^{n_v}$ is the reference input and $y(k) \in \mathbb{R}^{n_y}$ is the constrained output vector which must satisfy

$$y(k) \in \mathscr{Y} = \{y \,:\, y \leq h, \quad h \geq 0\}. \tag{3}$$

The conventional ECG (introduced by Gilbert and Ong (2011)) generates the reference input $v(k)$ based on the auxiliary subsystem:

$$\begin{aligned} x_a(k+1) &= A_a x_a(k), \\ v(k) &= C_a x_a(k)+\rho(k), \\ \rho(k+1) &= \rho(k), \end{aligned} \tag{4}$$

where $x_a(k) \in \mathbb{R}^{n_a}$.

Coupling (2) with the ECG (4), the augmented state, $\tilde{x} := [x^T, x_a^T]^T$, follows the following dynamics

$$\begin{aligned} \tilde{x}(k+1) &= \Psi\tilde{x}(k)+G\rho(k), \\ y(k) &= H\tilde{x}(k)+D\rho(k), \end{aligned} \tag{5}$$

with

$$\Psi = \begin{bmatrix} A & BC_a \\ O_{n_a} & A_a \end{bmatrix}, \quad G = \begin{bmatrix} B \\ O_{n_a,n_v} \end{bmatrix} \quad , \quad H = [C \; DC_a]. \tag{6}$$

Choosing A_a to be a Schur matrix and assuming A to be Schur (as 2 typically represents a nominal closed-loop system), it follows that Ψ is a Schur matrix. The conventional ECG relies on the characterization of the set of initial conditions $(\tilde{x}(0), \rho(0))$ that lead to responses which satisfy constraints (3) for all future time instants.

The response to an initial condition $\tilde{x}(0)$ and $\rho(0) := \rho$ is computed as:

$$y(k) = H\Psi^k\tilde{x}(0) + \left(H\sum_{i=0}^{k^*-1}\Psi^i G + D\right)\rho. \tag{7}$$

It is then possible to characterize a subset of constraint admissible pairs $(\tilde{x}(0), \rho)$ by stacking a finite number of inequality constraints:

$$\begin{bmatrix} H & D \\ \vdots & \vdots \\ H\Psi^k & H\sum_{i=0}^{k-1}\Psi^i G + D \\ \vdots & \vdots \\ H\Psi^{k^*} & H\sum_{i=0}^{k^*-1}\Psi^i G + D \\ O_{n_y,n_x+n_a} & H(I-\Psi)^{-1}G + D \end{bmatrix} \begin{bmatrix} \tilde{x}(0) \\ \rho \end{bmatrix} \leq \begin{bmatrix} h \\ \vdots \\ h \\ \vdots \\ h \\ (1-\varepsilon)h \end{bmatrix}, \tag{8}$$

where the last inequality holds when the steady state constrained output $(H(I-\Psi)^{-1}G+D)\rho$ strictly satisfies constraints with a margin determined by ε.

Note that k^*, ε, $0 < \varepsilon << 1$, are picked in agreement with the theoretical results in Gilbert and Ong (2011), which, under the assumptions that Ψ is Schur, (H, Ψ) is observable and $\mathscr{Y}$ is a compact and convex set with nonempty interior, guarantee the existence of a finite k^* such that the set $\tilde{O}_\infty$ defined by (8) is a positively invariant subset of the maximum constraint admissible set, O_∞.

Finally, given the commanded reference, r^*, at the time instant k, the ECG updates both $\rho(k)$ and the internal state $x_a(k)$ by solving a quadratic programming problem,

$$(\rho(k), x_a(k)) = \underset{\rho, x_a}{arg\,\min} \|r^* - \rho\|^2 + x_a^T Q x_a, \tag{9}$$

$$s.t \; (\tilde{x}(k), \rho) \in \tilde{O}_\infty \tag{10}$$

where $Q = Q^T > 0$ satisfies the discrete-time Lyapunov inequality,

$$A_a^T Q A_a - Q < 0. \tag{11}$$

The modified ECG command is then computed according to $v(k) = C_a x_a(k) + \rho(k)$.

2.2 Fast ECG synthesis in presence of an uncertain modeling parameter

The objective of this subsection is to propose a modification of the conventional ECG to a particular class of constrained discrete-time systems with a single parameter uncertainty. The study of such a class was motivated by our application which is detailed in the next section. The considered class of systems is thus of the form,

$$\begin{aligned} x(k+1) &= A(p)x(k)+B(p)v(k), \\ y(k) &= Cx(k)+Dv(k), \end{aligned} \tag{12}$$

where $k \in \mathbb{Z}^+$, $p \in \mathscr{P}_2$, the unit simplex in $\mathbb{R}^2$, $x(k) \in \mathbb{R}^{n_x}$ is the plant state, $v(k) \in \mathscr{R}^{n_v}$ is the reference input and $y(k) \in \mathbb{R}^{n_y}$ is the constrained output vector which must satisfy (3). In what follows, the notation $M(p)$ refers to a matrix which lies in the polytope $Co\{M_1, M_2\} := \{p_1M_1 + p_2M_2 \;,\; p_1, p_2 \geq 0 \;,\; p_1 + p_2 = 1\}$.

Consider now an ECG where $v(k)$ is generated by

$$\begin{aligned} x_a(k+1) &= A_a x_a(k), \\ v(k) &= C_a x_a(k)+\rho(k), \\ \rho(k+1) &= \lambda\rho(k), \end{aligned} \tag{13}$$

and where $x_a \in \mathbb{R}^{n_a}$ and $0 < \lambda < 1$.

Coupling (12) with the ECG (13), the augmented state, $\tilde{x} := [x^T, x_a^T]^T$, follows the following dynamics,

$$\begin{aligned} \tilde{x}(k+1) &= \Xi(p)\tilde{x}(k)+G(p)\rho(k), \\ y(k) &= H\tilde{x}(k)+D\rho(k), \end{aligned} \tag{14}$$

with:

$$\Xi_1 = \begin{bmatrix} A_1 & B_1C_a \\ O_{n_a} & A_a \end{bmatrix} \quad , \quad \Xi_2 = \begin{bmatrix} A_2 & B_2C_a \\ O_{n_a} & A_a \end{bmatrix} \quad , \quad G_1 = \begin{bmatrix} B_1 \\ O_{n_a,n_v} \end{bmatrix} \tag{15}$$

$$G_2 = \begin{bmatrix} B_2 \\ O_{n_a,n_v} \end{bmatrix}, \quad H = [C \; DC_a]. \tag{16}$$

Remark 1. Note that unlike (4), $\lambda < 1$ is used in (13). As further discussed, this allows to handle time-varying constraints whose rate of change is less than λ. This approach was also introduced for conventional reference governor in Kalabić and Kolmanovsky (2014) to handle the cases when the reference and/or the constraints are time-varying.

To simplify the notations, we add ρ to the extended state so that $\tilde{x}_\rho := [x^T, x_a^T, \rho^T]^T$ follows the following dynamics,

$$\begin{aligned} \tilde{x}_\rho(k+1) &= \Phi(p)\tilde{x}_\rho(k), \\ y(k) &= H_\rho\tilde{x}_\rho(k). \end{aligned} \tag{17}$$

Let us now consider the problem of computing the set O_∞, when p is unknown. Such a problem has been considered in Casavola et al. (2000) and Pluymers et al. (2005). The key ingredient (based on the main result of Barmish and Sankaran (1979)) was to observe that

$$\Phi(p)^k \in Co\left\{\prod_{j=0}^{k-1}\Phi_{i_j}, \forall i_j \in \{1,2\}\right\}, \tag{18}$$

which is the convex hull of all possible products of k matrices chosen in $\{\Phi_1, \Phi_2\}$.

It is then possible to characterize a subset of constraint admissible pairs $(\tilde{x}(0),\rho(0))$ by stacking a finite number of inequality constraints as in (8) where H is replaced by $H_{\rho,k}$ in the kth constraint, which is recursively defined by (Pluymers et al. (2005),Theorem 1) as

$$H_{\rho,k} = \begin{bmatrix} H_{\rho,k-1}\Phi_1 \\ H_{\rho,k-1}\Phi_2 \end{bmatrix}, \tag{19}$$

with $H_{\rho,0} := H_\rho$, and where the last inequality holds when the steady state constrained output $T\rho = H(I-\Xi(p))^{-1}G(p)\rho + D\rho$ (which is here supposed to be independent from p) satisfies constraints with margin ε.
Note that k^*, ε, $0<\varepsilon<1$, are picked in agreement with the theoretical results (Lemma 1 in Casavola et al. (2000)) which require, for all $p\in\mathscr{P}_2$, $\Xi(p)$ to be Schur, $(H,\Xi(p))$ to be observable and $\mathscr{Y}$ to be a compact and convex set with nonempty interior.

Remark 2. Note that an assumption that T does not depend on p is reasonable in many applications. This assumption is satisfied by the linearized guidance dynamics of the aircraft which will be detailed in the next section.

The previous developments apply even when the parameter p is time-varying. In the case when p is a constant unknown parameter, rather than computing all the possible products of k matrices chosen in $\{\Phi_1,\Phi_2\}$, the computational burden can be significantly decreased if one uses the following result in place of (18):

Lemma 1. Let k and $i\le k$ be two integers. Let σ be an operator recursively defined as follows:

- When $k=0$, $\sigma(\Phi_1^0,\Phi_2^0)=I$.
- When $k\ge 1$, and $\forall i\in[1,k]$

$$\sigma(\Phi_1^{k+1},\Phi_2^0) = \Phi_1^{k+1}, \tag{20}$$
$$\sigma(\Phi_1^0,\Phi_2^{k+1}) = \Phi_2^{k+1}, \tag{21}$$
$$\sigma(\Phi_1^{k+1-i},\Phi_2^i) = \sigma(\Phi_1^{k-i},\Phi_2^i)\Phi_1 + \sigma(\Phi_1^{k+1-i},\Phi_2^{i-1})\Phi_2. \tag{22}$$

Then, $\forall p\in\mathscr{P}_2$, $\forall k\in\mathbb{N}$:

$$\Phi(p)^k \in Co\left\{\frac{1}{C_k^i}\sigma(\Phi_1^{k-i},\Phi_2^i), i\in[0,k]\right\}. \tag{23}$$

where C_k^i denote the binomial coefficients.

Proof: First, one can easily recursively prove the following properties: $\forall(\theta_1,\theta_2)\in\mathbb{R}^2$,

$$\sigma((\theta_1\Phi_1)^{k-i},\Phi_2^i) = \theta_1^{k-i}\sigma(\Phi_1^{k-i},\Phi_2^i), \tag{24}$$
$$\sigma(\Phi_1^{k-i},(\theta_2\Phi_2)^i) = \theta_2^i\sigma(\Phi_1^{k-i},\Phi_2^i), \tag{25}$$
$$(\theta_1\Phi_1+\theta_2\Phi_2)^k = \sum_{i=0}^{k}\theta_1^{k-i}\theta_2^i\sigma(\Phi_1^{k-i},\Phi_2^i). \tag{26}$$

We then introduce the normalized function $\bar{\sigma}$ defined by

$$C_k^i\bar{\sigma}(\Phi_1^{k-i},\Phi_2^i) = \sigma(\Phi_1^{k-i},\Phi_2^i), \tag{27}$$

in order to rewrite (26) as follows

$$(\theta_1\Phi_1+\theta_2\Phi_2)^k = \sum_{i=0}^{k}C_k^i\theta_1^{k-i}\theta_2^i\bar{\sigma}(\Phi_1^{k-i},\Phi_2^i). \tag{28}$$

It is then readily seen that when one chooses $\theta_1,\theta_2\ge 0$ such that $\theta_1+\theta_2=1$, one has:

$$(\theta_1+\theta_2)^k = \sum_{i=0}^{k}C_k^i\theta_1^{k-i}\theta_2^i = 1. \tag{29}$$

The result (23) immediately follows from (28) and (29).

Remark 3. The result (23) essentially follows from the binomial formula. It could be generalized to unknown vectors $p\in\mathbb{R}^{n_p}$ using the multinomial formula. Note that the σ operator was introduced because the matrix multiplication is noncommutative.

Remark 4. Note that (18) is the convex hull of $n_y\times 2^k$ matrices whereas (23) is the convex hull of $n_y\times(k+1)$ matrices.

Consider now a set S determined by (8) in which H is replaced by $\Gamma_{\rho,k}$ with

$$\Gamma_{\rho,k} = D_k^{-1}\left(\begin{bmatrix} D_{k-1}\Gamma_{\rho,k-1} \\ O_{n_x+n_a+n_v}\end{bmatrix}\Phi_1 + \begin{bmatrix} O_{n_x+n_a+n_v} \\ D_{k-1}\Gamma_{\rho,k-1}\end{bmatrix}\Phi_2\right), \tag{30}$$

and

$$D_k := Blkdiag\left(\left[C_k^i I_{n_x+n_a+n_v}, i=0\dots k\right]\right). \tag{31}$$

There exists k^* such that set S is a strongly returnable subset of the maximum output admissible set for system (17) and constraints (3). Clearly, S is a subset of O_∞ since any $\Phi(p)^k$ satisfying (23) satisfies (18) too. The existence of k^* is guaranteed by the same ingredients which ensure finite determination property of O_∞. Now, observe that since $0<\lambda<1$, Φ is strictly Schur and as a consequence, for all $(\tilde{x}(0),\rho(0))\in S$, $(\tilde{x}(k),\rho(k))$ asymptotically tends to $0\in Int(S)$. Then, as S is compact, there exists a time instant after which $(\tilde{x},\rho)$ remains in S.

Remark 5. S being non invariant, the optimization problem (9) may not admit a solution at some step k. In this case, simply applying $x_a(k)=A_a x_a(k-1)$, $\rho(k)=\lambda\rho(k-1)$ ensures that the constraints are satisfied since $S\subset O_\infty$.

3. APPLICATION TO VISION-BASED LANDING

3.1 Scenario

The landing of an airliner is one of the most critical phases of flight. Ground systems (ILS/GBAS) enabling assisted landings are today the main way to ease the piloting task during this phase. Thanks to these systems, the deviations of the aircraft with respect to the runway can be computed and used in the guidance laws. However, such systems are expensive and their availability is limited to airports having deployed the required infrastructure. Moreover, urgent landings are by definition made without such help.
Consequently, systems that only rely on embedded sensors are of interest. In this paper, we consider the use of an embedded monocular camera, which was the focus of the VISIOLAND project funded by the French National Research Agency between 2013 and 2017.

3.2 Notation

In this work, we focus on the alignment phase (also called approach phase) during which an autopilot system must reach and maintain a constant glide slope $\gamma^d=-3\ deg$ at a constant airspeed $V=72ms^{-1}$ (which corresponds to 140 knots). The following variables are defined (See figure 1):

- $\Delta_X,\Delta_Y,\Delta_Z$ are the components of the position vector between the aircraft center of gravity (as a first approximation, the camera is supposed to be placed at this point) and the runway touchdown point.

- γ, ψ, φ are the relative slope, yaw and roll angles between the aircraft and the runway.

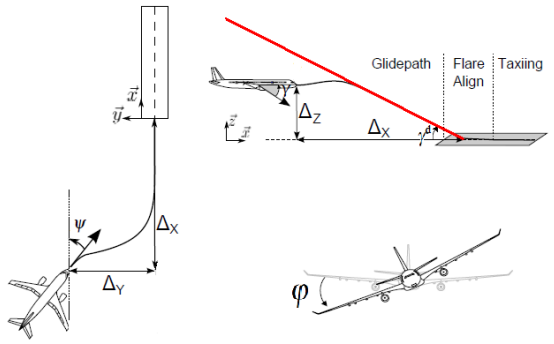

Fig. 1. Notations used in the alignment phase

Remark 6. The flare phase follows the alignment phase and precedes the touchdown and roll-out phases of landing. Although our work is focused on the alignment phase, some state constraints will be added in the sequel so that the flare phase can start in the required conditions.

3.3 Aircraft dynamical model

Using the aforementioned notation, the guidance dynamics of an aircraft during a descent at a constant speed V are described by

$$\begin{cases} \dot{\Delta}_X = V\cos(\psi)\cos(\gamma), \\ \dot{\Delta}_Y = V\sin(\psi)\cos(\gamma), \\ \dot{\Delta}_Z = V\sin(\gamma), \\ \dot{\psi} = \dfrac{g}{V}\tan(\varphi), \\ \dot{\gamma} = \dfrac{g}{V}u_{long}, \\ \dot{\varphi} = u_{lat}. \end{cases} \tag{32}$$

where u_{long} and u_{lat} are the control inputs. Note that the inner loop of EFCS (Electronic flight control systems) involved in generating u_{long} and u_{lat} is not taken into account in this study.

3.4 Visual measurements

In the aforementioned VISIOLAND project, the most stringent scenario from the control point of view is the vision-based landing of an aircraft on an unequipped runway whose size is partially unknown. More precisely, the runway is unequipped in the sense that there are no landing ground facilities as ILS (Instrument Landing System) or GPS (Global Positioning System). In such circumstances, the automatic guidance loop relies merely on embedded sensors which, in this case, are a monocular camera and an IMU (Inertial Measurement Unit). Assuming the runway is not inclined, the relative attitude angles $y_5 = \gamma$ and $y_6 = \varphi$ are simply the aircraft's flight path and roll angles, thus given by the IMU.
Let us now define the following quantities:

$$y_1 = \frac{\Delta_Z}{\Delta_X} \quad , \quad y_2 = \frac{w}{\Delta_X} \quad , \quad y_3 = \frac{\Delta_Y}{\Delta_X}. \tag{33}$$

where w is the runway width.
Assuming the runway is kept inside the camera field of view all along the descent, it was shown in Burlion and de Plinval (2017a,b) that the relative yaw angle $y_4 = \psi$ and the visual outputs (33) can be obtained by image processing from the body fixed camera.

Suppose now that the aircraft is landing on a runway which is only partially unknown in the sense that its width lies in a given interval [1], which is typically [30m, 60m]. In other words,

$$w \in Co\{30, 60\}. \tag{34}$$

Note that its inverse w^{-1} lies in the interval $[1/60, 1/30]$ and its mean value is $1/40$.
Also observe that the deviation with respect to the glide slope in the longitudinal frame can be expressed as

$$\delta_Z = \Delta_Z - \tan(\gamma^d)\Delta_X. \tag{35}$$

Assuming that Δ_X never crosses 0 in the considered glide phase, we easily deduce from (33) and (34) that

$$40\frac{y_1 - \tan(\gamma^d)}{y_2} = \frac{40}{w}\delta_Z \in Co\left\{\frac{2}{3}\delta_Z, \frac{4}{3}\delta_Z\right\} \tag{36a}$$

$$40\frac{y_3}{y_2} = 40\frac{\Delta_Y}{w} \in Co\left\{\frac{2}{3}\Delta_Y, \frac{4}{3}\Delta_Y\right\} \tag{36b}$$

These two quantities are further exploited by the guidance control laws.

3.5 Linearized closed-loop longitudinal aircraft dynamic model and ECG formulation

Continuous-time open loop dynamics. Using the available visual measurements (33) and the knowledge of the runway width (34), we have obtained the estimate (36a). Define the state vector for the longitudinal linearized dynamics as

$$x_{long} = \left[40\frac{y_1 - \tan(\gamma^d)}{y_2},\ \gamma - \gamma^d\right]^T = \left[\left(\frac{2}{3}p_1 + \frac{4}{3}p_2\right)\delta_Z,\ \delta_\gamma\right]^T, \tag{37}$$

where $\delta_\gamma = \gamma - \gamma^d$, and the control input as

$$u_{long} = N_z - 1, \tag{38}$$

where N_z is the vertical load factor expressed in g units and 1 g is the acceleration due to gravity (typically $g = 9.81 m.s^{-2}$). As an example, when the velocity magnitude equals $V = 72\ m.s^{-1}$, the linearization of (32) around $[0, \gamma^d, 0, 0, 0]'$ projected on the longitudinal frame is given by

$$\dot{x}_{long} = A_{long}(p)x_{long} + B_{long}u_{long}, \tag{39}$$

where

$$A_{long}(p) = \begin{bmatrix} 0 & 72(0.66p_1 + 1.33p_2) \\ 0 & 0 \end{bmatrix}, \quad B_{long} = \begin{bmatrix} 0 \\ 0.134 \end{bmatrix}. \tag{40}$$

Longitudinal nominal controller. The longitudinal controller is a state feedback control law augmented with a feedforward signal v_{long},

$$u_{long} = -K_{long}x_{long} + K^1_{long}v_{long}, \tag{41}$$

in which, v_{long} is the output of the ECG longitudinal loop, and

$$K_{long} = [K^1_{long}, K^2_{long}] = [0.0016\ \ 1.6043], \tag{42}$$

was obtained using pole placement in the absence of visual outputs (i.e., for the nominal case where $p_1 = p_2 = \frac{1}{2}$).
Applying the control law (41) to the dynamics (39), the closed-loop system is of the form:

$$\dot{x}_{long} = A^c_{long}(p)x_{long} + B_{v,long}v_{long}, \tag{43}$$

where $A^c_{long}(p) = A_{long}(p) - B_{long}K_{long} := p_1A^c_{long,1} + p_2A^c_{long,2}$ and $B_{v,long} := B_{long}K^1_{long}$.

[1] The uncertainty therefore comes from the width of the runway that is not known in advance in case of emergency. One could argue that a runway database might be available, but such a database is not currently certified.

Discretized longitudinal closed-loop model. Given a sampling period of $\Delta_T = 1$ s, [2] the uncertain closed loop system is approximated by the following discrete-time model,

$$x_{long}(k+1) = A^d_{long}(p)x_{long}(k) + B^d_{v,long}(p)v_{long}(k), \quad (44)$$

where for $i \in \{1,2\}$

$$A^d_{long,i} = e^{\Delta_T A^c_{long,i}}, \quad (45)$$

and

$$B^d_{v,long,i} = (A^c_{long,i})^{-1}\left(e^{\Delta_T A^c_{long,i}} - I_2\right)B_{v,long}. \quad (46)$$

Remark 7. Note that (44) is an approximation and not the result of the exact conversion of (43) to discrete-time. Subsequent simulations will validate the control design on the original nonlinear continuous-time model.

Remark 8. Note that the nominal control law (41) is designed on the nominal model. It is then numerically checked that $A^d_{long}(p)$ is a Schur matrix $\forall p \in \mathscr{P}_2$. To do that, we simply checked that the eigenvalues of $A^d_{long}(p)$ lie in the unit circle for a large selection of parameters $p \in \mathscr{P}_2$.

Selection of the ECG internal dynamics. As discussed in Gilbert and Ong (2011) and Kalabic et al. (2011), there exist many possibilities to choose the auxiliary dynamics (4). Here, we use a Laguerre's sequence generator with

$$A_{a,long} = \begin{bmatrix} \alpha_{long} & \beta_{long} \\ 0 & \alpha_{long} \end{bmatrix} \quad , \quad C_{a,long} = \sqrt{\beta_{long}}\,[1 \;\; -\alpha_{long}], \quad (47)$$

where $\beta_{long} = \sqrt{1-\alpha_{long}}$, $\alpha_{long} = 0.8$. Note that α_{long} was selected as the value which gives the largest O_∞ sets when $p = [1\ 0]$ and $p = [0\ 1]$. We also tested the shift register generator that corresponds to $\alpha_{long} = 0$, $\beta_{long} = 1$ which did not give larger O_∞ sets.

3.6 Linearized closed-loop lateral aircraft dynamic model and ECG formulation

Continuous-time open loop model. Due to the use of available visual information (36a) and of the IMU, the state vector for the lateral linearized dynamics is defined as

$$x_{lat} = \left[40\frac{y_3}{y_2},\ \psi,\ \varphi\right]^T = \left[\left(\frac{2}{3}p_1 + \frac{4}{3}p_2\right)\Delta_Y,\ \psi,\ \varphi\right]^T, \quad (48)$$

and the control input is defined as

$$u_{lat} = \dot{\varphi}. \quad (49)$$

As an example, when the aircraft velocity magnitude equals $V = 72\ m.s^{-1}$, the linearization of (32) around $[0, \gamma^d, 0, 0, 0]'$ projected on the lateral frame is given by

$$\dot{x}_{lat} = A_{lat}(p)x_{long} + B_{lat}u_{lat}, \quad (50)$$

where

$$A_{lat}(p) = \begin{bmatrix} 0 & 72\left(\frac{2}{3}p_1 + \frac{4}{3}p_2\right) & 0 \\ 0 & 0 & 0.137 \\ 0 & 0 & 0 \end{bmatrix}, \quad B_{lat} = \begin{bmatrix} 0 \\ 0 \\ 1 \end{bmatrix}. \quad (51)$$

Lateral nominal controller. The lateral controller is a state feedback control law augmented with a feedforward signal v_{lat},

$$u_{lat} = -K_{lat}x_{lat} + K^1_{lat}v_{lat}, \quad (52)$$

in which v_{lat} is the output of the ECG lateral loop, and

$$K_{lat} = [K^1_{lat}, K^2_{lat}] = [0.003\ \ 2.22\ \ 0.985], \quad (53)$$

[2] This choice is further discussed in Remark 10.

was obtained using pole placement in the absence of visual outputs (i.e., for the nominal case when $p_1 = p_2 = \frac{1}{2}$).
The closed loop system is thus represented by the following linear model,

$$\dot{x}_{lat} = A^c_{lat}(p)x_{lat} + B_{v,lat}v_{lat}, \quad (54)$$

where $A^c_{lat}(p) = A_{lat}(p) - B_{lat}K_{lat} := p_1A^c_{lat,1} + p_2A^c_{lat,2}$ and $B_{v,lat} := B_{lat}K^1_{lat}$.

Discretized lateral closed loop model. In analogy to subsection 3.5.3, the discrete-time lateral closed loop system model is given by

$$x_{lat}(k+1) = A^d_{lat}(p)x_{lat}(k) + B^d_{v,lat}(p)v_{lat}(k), \quad (55)$$

where for $i \in \{1,2\}$

$$A^d_{lat,i} = e^{\Delta_T A^c_{lat,i}}, \quad (56)$$

and

$$B^d_{v,lat,i} = (A^c_{lat,i})^{-1}\left(e^{\Delta_T A^c_{lat,i}} - I_2\right)B_{v,lat}. \quad (57)$$

Remark 9. In line with Remark 8, we numerically checked that $A^d_{lat}(p)$ is Schur for all $p \in \mathscr{P}_2$.

Selection of the ECG internal dynamics. In analogy with subsection 3.5.4, we use a Laguerre's sequence generator with

$$A_{a,lat} = \begin{bmatrix} \alpha_{lat} & \beta_{lat} & -\alpha_{lat}\beta_{lat} \\ 0 & \alpha_{lat} & \beta_{lat} \\ 0 & 0 & \alpha_{lat} \end{bmatrix}, C_{a,lat} = \sqrt{\beta_{lat}}\begin{bmatrix} 1 & -\alpha_{lat} & \alpha^2_{lat} \end{bmatrix}, \quad (58)$$

where $\beta_{lat} = \sqrt{1-\alpha_{lat}}$, $\alpha_{lat} = 0.8$.

3.7 State and control constraints

Within the aforementioned VISIOLAND project, AIRBUS proposed to study merely the guidance loops but imposed a set of constraints so that the obtained model still captures the features of a more complex model, which would contain the inner loop in conjunction with some sophisticated flight envelope protection laws (which usually act at the control surface deflection level). In fact, the control design process used by AIRBUS relies on increasing higher fidelity aircraft models as dictated by the standardized industrial V&V process, see Goupil et al. (2014). Consequently, the problem treated here can be viewed as the first step in an industrial control development and certification process.

As such, some control constraints are first imposed on the two control inputs of the guidance loops. In our numerical examples, these constraints are of the form,

$$-1\ g \leq u_{long} \leq 2\ g, \quad (59)$$

$$-12\ deg.s^{-1} \leq u_{lat} \leq 12\ deg.s^{-1}. \quad (60)$$

Some safety constraints are imposed on the fight path angle and roll angle as

$$-6\ deg \leq \gamma \leq 10\ deg, \quad (61)$$

$$-66\ deg \leq \varphi \leq 66\ deg. \quad (62)$$

Finally, following the approach of Metni et al. (2003), an additional constraint is imposed on the yaw error ψ in order to limit the aircraft orientation and thus keep the runway in the camera field of view. In our numerical examples, the constraint is imposed as:

$$-30\ deg \leq \psi \leq 30\ deg. \quad (63)$$

3.8 Landing constraints

In order to softly land on the runway, the aircraft does not need to perfectly follow the glide slope at the end of the align phase but must respect some constraints to be able to correctly perform the flare.

Computation of the minimum number of time steps required before starting the flare phase. For the linearized aircraft dynamics, the evolution of the signed distance $\Delta_X \leq 0$ to the touchdown point can be modelled as

$$\dot{\Delta}_X = V = 72m/s, \tag{64}$$

which, in discrete time, is written as

$$\Delta_X(k+1) = \Delta_X(k) + \Delta_T 72 = \Delta_X(k) + 72. \tag{65}$$

Usually, the flare phase starts when $\Delta_X(\bar{k}) \cong -200$m. In this case, $\bar{k}$ is the minimum integer such that

$$-200 \leq \Delta_X(0) + 72\bar{k}. \tag{66}$$

Due to the fact that the runway width is imprecise, Δ_X is known up to a ratio. Indeed, using (33)-(34) plus the fact that $y_2 \leq 0$ one has that $\Delta_X \in Co\{\frac{60}{y_2}, \frac{30}{y_2}\}$. As such, $\bar{k}$ must satisfy the following inequality,

$$-200 \leq \frac{30}{y_2(0)} + 72\bar{k}, \tag{67}$$

which finally gives the following estimate for the number of time steps before starting the flare phase,

$$\bar{k} = round\left(\frac{-\frac{30}{y_2(0)} - 200}{72}\right). \tag{68}$$

Definition of time-varying constraints to softly land the aircraft.
If we assume that the flare phase will not start before $\bar{k} \in \mathbb{N}$ iterations, then the constraints have the following form,

$$-22\ m \leq \quad \Delta_Y(k \geq \bar{k}) \quad \leq 22\ m, \tag{69}$$
$$-7.5\ m \leq \quad \delta_Z(k \geq \bar{k}) \quad \leq 7.5\ m, \tag{70}$$
$$-3\ deg \leq \gamma(k \geq \bar{k}) - \gamma^d \leq 3\ deg, \tag{71}$$
$$-15\ deg \leq \quad \psi(k \geq \bar{k}) \quad \leq 15\ deg, \tag{72}$$
$$-5\ deg \leq \quad \varphi(k \geq \bar{k}) \quad \leq 5\ deg. \tag{73}$$

Given of (48) and (37), it can be shown that these constraints will be satisfied if the following state constraints are satisfied element-wise

$$-\bar{x}_{long}(\bar{k}) \leq x_{long}(k \geq \bar{k}) \leq \bar{x}_{long}(\bar{k}), \tag{74}$$
$$-\bar{x}_{lat}(\bar{k}) \leq x_{lat}(k \geq \bar{k}) \leq \bar{x}_{lat}(\bar{k}), \tag{75}$$

where

$$\bar{x}_{long}(\bar{k}) := \begin{bmatrix} \frac{2}{3}\bar{\delta}_Z \\ \bar{\delta}_\gamma \end{bmatrix} = \begin{bmatrix} 5\ m \\ 3\ deg \end{bmatrix}, \bar{x}_{lat}(\bar{k}) := \begin{bmatrix} \frac{2}{3}\bar{\Delta}_Y \\ \bar{\psi} \\ \bar{\varphi} \end{bmatrix} = \begin{bmatrix} 14.6\ m \\ 15\ deg \\ 5\ deg \end{bmatrix}. \tag{76}$$

Such constraints can be transformed to '$if(k \geq \bar{k}) - then$' type constraints, which has the following disadvantages:

- the computation of the strongly returnable set requires at least $\bar{k}$ iterations,
- the computed strongly returnable sets will depend on $\bar{k}$. As such, this complicates the design if $\bar{k}$ is not known in advance since many sets must be stored,
- the terminal constraints suddenly appear and may cause the ECG to react abruptly.

As a remedy, we now propose a different approach which consists in replacing these constraints by time-varying constraints. Inspired by the work of Kalabić and Kolmanovsky (2014), our idea is to choose the rate of change of the constraints according to the unconstrained closed loop dynamics. Roughly speaking, we impose the constraints not to vary faster than the unconstrained closed-loop system.
As such, let us first compute the largest spectral radius $\lambda_{long} \in]0,1[$ (resp. $\lambda_{lat} \in]0,1[$) of the uncertain longitudinal (resp. lateral) closed loop dynamics $A^d_{long}(p)$ (resp. $A^d_{lat}(p)$) for all $p \in \mathscr{P}_2$.
When $\Delta_T = 1s$, we compute:

$$\lambda_{long} = 0.935, \quad \lambda_{lat} = 0.913. \tag{77}$$

We then define the following time-varying bounds

$$\bar{x}_{long}(k) = \lambda_{long}^{k-\bar{k}} \bar{x}_{long}(\bar{k}) \quad , \quad \bar{x}_{lat}(k) = \lambda_{lat}^{k-\bar{k}} \bar{x}_{lat}(\bar{k}). \tag{78}$$

It is clear that if for all $k \in \mathbb{N}$, the following constraints are satisfied

$$-\bar{x}_{long}(k) \leq x_{long}(k) \leq \bar{x}_{long}(k), \quad -\bar{x}_{lat}(k) \leq x_{lat}(k) \leq \bar{x}_{lat}(k), \tag{79}$$

then (74), (75) are satisfied.
Figure 2 illustrates the transformation of the (black colored) interval constraint $[\underline{z}(\bar{k}), \bar{z}(\bar{k})]$ on a variable z at time $k \geq \bar{k}$ into some (red-colored) time-varying constraints.

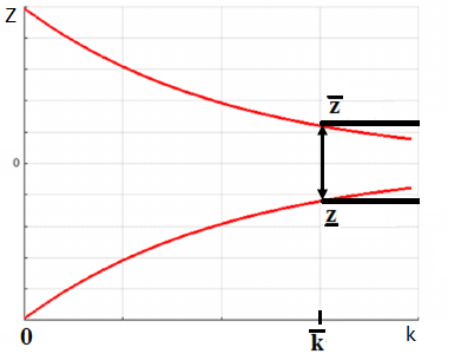

Fig. 2. From an interval to time-varying constraints

Remark 10. Note that $\bar{k}$ depends on Δ_T which means that the number of inequalities (which define the strongly returnable set) depends on Δ_T when $k^* \geq \bar{k}$. The choice of $\Delta_T = 1$ s was made in our numerical simulations.

ECG design in presence of time-varying constraints. It is easy to see that the time-varying bounds (78) satisfy

$$\bar{x}_{long}(k+1) = \lambda_{long}\bar{x}_{long}(k), \quad \bar{x}_{lat}(k+1) = \lambda_{lat}\bar{x}_{lat}(k). \tag{80}$$

Then, these time varying constraints are taken into account by simply augmenting the system state with $\bar{x}_{long}$ and $\bar{x}_{lat}$. Doing so, the time-varying bounds (79) become simple linear constraints on the extended state. However, to accommodate such bounds tending to 0, we considered the unconventional use of $\lambda \neq 1$ in the ECG dynamics (13).

4. NUMERICAL RESULTS

In this section, we construct the strongly returnable sets which are used to implement the ECG. We first discuss algorithmic

methods for reducing the complexity and then provide simulation results. The method is finally validated on the continuous-time nonlinear guidance dynamics of the aircraft.

4.1 Linearized model simulation

Computation of the strongly returnable sets. As discussed in Section 2, the binomial formula enables to drastically alleviate the computational burden. However, the number of inequality constraints which define the strongly returnable sets is still significant. Let us use the time horizon $k_{\max} = 35$; since the algorithm did not stop before $k = k_{\max}$ (which means that the theoretical bound $k^* \geq k_{\max}$), one obtains 6888 (resp. 10332) non redundant inequalities for the longitudinal (resp. lateral) strongly returnable set denoted by S_{long} (resp. S_{lat}). Using the procedure described in Gilbert and Kolmanovsky (1999), we then approximated these sets as follows.

- We eliminated the almost redundant constraints. Using $\varepsilon = 0.025$, we obtain an outer approximation $S_{long,\varepsilon}$ of S_{long} (resp. $S_{lat,\varepsilon}$) based now on 286 (resp. 1110) non redundant inequality constraints,
- We used a pull-in procedure to guarantee the constraint satisfaction despite these approximations. For instance in the longitudinal frame, using linear programming, we computed the largest value of $\alpha \geq 1$ such that $S_{long,\alpha} := \{x\ ,\ \alpha H_{long,\varepsilon} x \leq h_{long,\varepsilon}\} \subset S_{long} := \{x\ ,\ H_{long} x \leq h_{long}\}$ where $S_{long,\varepsilon} := \{x\ ,\ H_{long,\varepsilon} x \leq h_{long,\varepsilon}\}$. We obtained $\alpha = 1.16$ (resp. 1.27 for the lateral frame).

Illustration. Let us consider now the following scenario: the aircraft is approaching and a runway appears in the video camera image at a time $t = 0$; the runway is assumed to remain inside the field of view of the camera in the sequel. Then, $\bar{k} = 35$ is computed using (68). We also compute $\bar{x}_{long}(0)$ and $\bar{x}_{lat}(0)$ using (78). Using these values, we can compute the set of initial conditions from which it is possible to perform the vision-based automatic landing while respecting all the constraints.
For instance, in the longitudinal frame and using the notation of the previous subsection, we computed the following sets

$$S_{long}^{ECG,\bar{k}=35} := \Big\{ (x_{long}(0), x_{a,long(0)}, \rho_0)\ :\ \alpha H_{long,\varepsilon} [x_{long}(0)^T, x_{a,long}(0)^T, \rho_0, \bar{x}_{long}(0)^T]^T \leq h_{long} \Big\}, \tag{81}$$

$$S_{long}^{RG,\bar{k}=35} := \Big\{ (x_{long}(0), \rho_0)\ :\ \alpha H_{long,\varepsilon} [x_{long}(0)^T, O_{1,n_a}, \rho_0, \bar{x}_{long}(0)^T]^T \leq h_{long} \Big\}, \tag{82}$$

and

$$S_{long}^{0,\bar{k}=35} := = \Big\{ (x_{long}(0)\ :\ \alpha H_{long,\varepsilon} [x_{long}(0)^T, O_{1,n_a}, 0, \bar{x}_{long}(0)^T]^T \leq h_{long} \Big\}, \tag{83}$$

for the ECG, conventional RG and no RG.
The projection S of these sets on the plane defined by x_{long} coordinates give the set of initial conditions from which the closed loop system will respect the constraints using an ECG (resp. a RG) (resp. no RG). In the longitudinal frame, Figure 3 shows these projections. The ECG-based set (shown in blue) is clearly larger that the RG-based one (shown in green). Note that the smaller set (shown in yellow) is the set obtained without any governor.

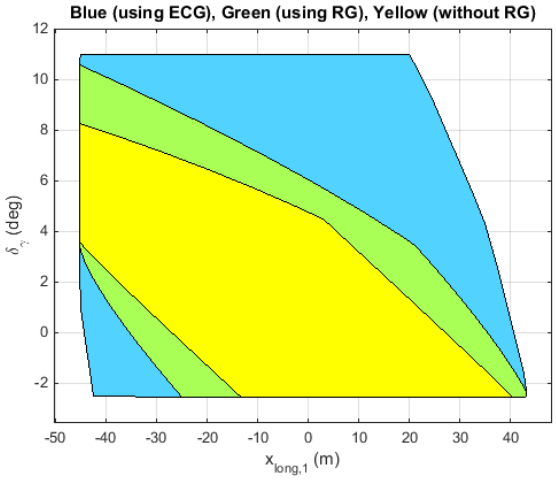

Fig. 3. Projections of the longitudinal strongly returnable sets (longitudinal frame).

Simulations on the linearized discretized models. Figure 4 illustrates the output response obtained using the ECG in he longitudinal frame. Similar results were obtained in the lateral frame. It can be confirmed that all the constraints are satisfied when the simulations start with initial conditions in the projections of strongly returnable sets represented (in blue) in Figure 3.

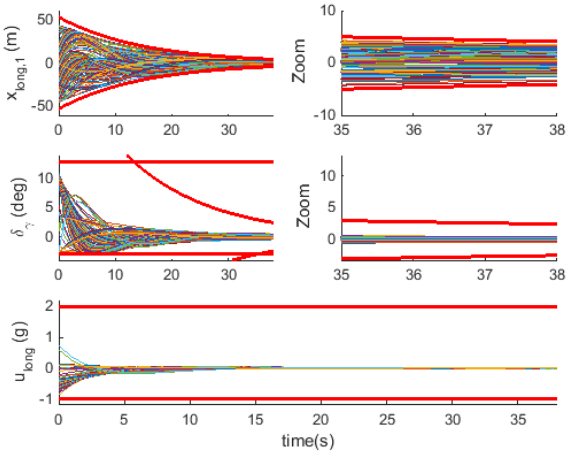

Fig. 4. The time histories of constrained outputs and constraints (red) as the initial values of $x_{long,1}$ and δ_{γ} vary in the computed strongly returnable set (longitudinal frame).

4.2 Nonlinear model simulation

As discussed previously, the efficient computation of a robust strongly returnable safe set was rendered possible by linearizing the guidance dynamics and using a sufficiently large sampling period $\Delta_T = 1s$ in converting the models to discrete-time. We validated our approach by performing additional simulations on the nonlinear continuous time guidance model, with ECG being updated every Δ_T seconds . The scenario is the one considered before (i.e, with $\bar{k} = 35$).

Simulation results. Figure 5 illustrates the output response obtained using the ECG with the nonlinear model. Looking at all the state variables, we verified that all the constraints are satisfied with the initial state when the simulations start in the projection of the strongly returnable set despite the fact that simulations are performed using the nonlinear continuous time model.

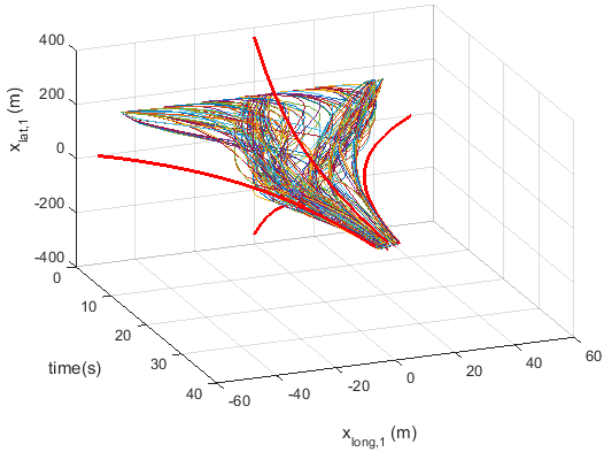

Fig. 5. Examples of 3D trajectories all starting from $x_{lat,1}(0) = 150$ m as the initial values of $x_{long,1}(0)$ and attitude vary in the computed strongly returnable sets. Constraints are shown by red curves.

5. CONCLUSIONS

In this paper, we have proposed a novel vision-based constrained guidance scheme to execute aircraft landing on a runway whose width is not precisely known. The solution is based on an extended command governor which operates by exploiting off-line computed robust strongly returnable sets. Such sets are computed efficiently by using a binomial expansion. The second main ingredient of our method is to transform the terminal constraints into appropriately defined time-varying constraints. This avoids the abrupt imposing of constraints and produces smoother responses. Future work could consider additional source of uncertainty like external disturbances or uncertain modelling parameters.

ACKNOWLEDGEMENT

The research of Laurent Burlion was supported by the French Ministry of Defense (DGA-MRIS). The research of Ilya Kolmanovsky was supported by the National Science Foundation Grant Numbers 1931738 and 1904394.

REFERENCES

Barmish, B. and Sankaran, J. (1979). The propagation of parametric uncertainty via polytopes. *IEEE Transactions on Automatic Control*, 24(2), 346–349.

Bemporad, A. and Morari, M. (1999). Control of systems integrating logic, dynamics, and constraints. *Automatica*, 35(3), 407 – 427.

Burlion, L. and de Plinval, H. (2017a). Toward vision based landing of a fixed-wing uav on an unknown runway under some fov constraints. In *2017 International Conference on Unmanned Aircraft Systems (ICUAS)*, 1824–1832.

Burlion, L. and de Plinval, H. (2017b). Vision based anti-windup design with application to the landing of an airliner. In *20th IFAC World Congress*, 10482 – 10487.

Casavola, A., Mosca, E., and Angeli, D. (2000). Robust command governors for constrained linear systems. *IEEE Transactions on Automatic Control*, 45(11), 2071–2077.

Di Cairano, S. and Borrelli, F. (2016). Reference tracking with guaranteed error bound for constrained linear systems. *IEEE Transactions on Automatic Control*, 61(8), 2245–2250.

Gibert, V., Burlion, L., Chriette, A., Boada, J., and Plestan, F. (2015). New pose estimation scheme in perspective vision system during civil aircraft landing. *IFAC-PapersOnLine*, 48(19), 238 – 243. 11th IFAC Symposium on Robot Control, (SYROCO), 2015.

Gilbert, E. and Kolmanovsky, I. (2002). Nonlinear tracking control in the presence of state and control constraints: a generalized reference governor. *Automatica*, 38(12), 2063–2073.

Gilbert, E.G. and Tan, K.T. (1991). Linear systems with state and control constraints: the theory and application of maximal output admissible sets. *IEEE Transactions on Automatic Control*, 36(9), 1008–1020.

Gilbert, E. and Kolmanovsky, I. (1999). Fast reference governors for systems with state and control constraints and disturbance inputs. *International Journal of Robust and Nonlinear Control*, 9(15), 1117–1141.

Gilbert, E. and Ong, C. (2011). Constrained linear systems with hard constraints and disturbances: An extended command governor with large domain of attraction. *Automatica*, 47(2), 334–340.

Goupil, P., Boada-Bauxell, J., Marcos, A., Cortet, E., Kerr, M., and Costa, H. (2014). Airbus efforts towards advanced real-time fault diagnosis and fault tolerant control. In *19th IFAC World Congress*, 3471–3476.

Kalabić, U. and Kolmanovsky, I. (2014). Reference and command governors for systems with slowly time-varying references and time-dependent constraints. In *53rd IEEE Conference on Decision and Control*, 6701–6706.

Kalabic, U., Kolmanovsky, I., Buckland, J., and Gilbert, E. (2011). Reference and extended command governors for control of turbocharged gasoline engines based on linear models. In *2011 IEEE International Conference on Control Applications (CCA)*, 319–325.

Kolmanovsky, I., Kalabić, U., and Gilbert, E. (2012). Developments in constrained control using reference governors. In *4th IFAC Nonlinear Model Predictive Control Conference*, 282–290.

Metni, N., Hamel, T., and Fantoni, I. (2003). Visual servoing with orientation limits of a x4-flyer. In *2003 European Control Conference (ECC)*, 1804–1809.

Pluymers, B., Rossiter, J.A., Suykens, J.A.K., and Moor, B.D. (2005). The efficient computation of polyhedral invariant sets for linear systems with polytopic uncertainty. In *Proceedings of the 2005, American Control Conference, 2005*, volume 2, 804–809.

Rakovic, S.V., Grieder, P., Kvasnica, M., Mayne, D.Q., and Morari, M. (2004). Computation of invariant sets for piecewise affine discrete time systems subject to bounded disturbances. In *43rd IEEE Conference on Decision and Control (CDC)*, volume 2, 1418–1423.